

# 1 Stem cell memory EBV-specific T cells control post- 2 transplant lymphoproliferative disease and persist *in vivo*

3

4 Darya Palianina<sup>1†</sup>, Juliane Mietz<sup>2†</sup>, Claudia Stühler<sup>1</sup>, Brice Arnold<sup>1</sup>, Glenn Bantug<sup>1</sup>,  
5 Christian Münz<sup>3</sup>, Obinna Chijioke<sup>2,4\*</sup>, Nina Khanna<sup>1,5-6\*</sup>

6

7 <sup>1</sup>Department of Biomedicine, University and University Hospital Basel, Basel,  
8 Switzerland; <sup>2</sup>Cellular Immunotherapy, Institute of Experimental Immunology,  
9 University of Zurich, Zurich, Switzerland; <sup>3</sup>Viral Immunobiology, Institute of  
10 Experimental Immunology, University of Zurich, Zurich, Switzerland; <sup>4</sup>Institute of  
11 Pathology and Medical Genetics, University Hospital Basel, Basel, Switzerland;  
12 <sup>5</sup>Division of Infectious Diseases and Hospital Epidemiology, University Hospital Basel,  
13 Basel, Switzerland; <sup>6</sup>Corresponding Author; Hebelstrasse 20, 4056 Basel,  
14 Switzerland; Tel: +41 61 328 73 25; Email: [nina.khanna@usb.ch](mailto:nina.khanna@usb.ch).

†D.P. and J.M. contributed equally to this work and share first authorship.

\*N.K. and O.C. contributed equally to this work and share last authorship.

15

## 16 ABSTRACT

17

18 Adoptive T cell therapy (ACT), the therapeutic transfer of defined T cell immunity to  
19 patients, offers great potential in the fight against different human diseases including  
20 difficult-to-treat viral infections but response rates are still suboptimal. Very early  
21 differentiated stem cell memory T cells (T<sub>SCM</sub>) have superior self-renewal, engraftment,  
22 persistence, and anti-cancer efficacy, but their potential for anti-viral ACT remains  
23 unknown. Here, we developed a clinically-scalable protocol for expanding Epstein-  
24 Barr virus (EBV)-specific T<sub>SCM</sub>-enriched T cells with high proportions of CD4<sup>+</sup> T cells  
25 and broad EBV antigen coverage. These cells showed tumor control in a xenograft  
26 model of post-transplant lymphoproliferative disorder (PTLD) and were superior to  
27 previous ACT protocols in terms of tumor infiltration, *in vivo* proliferation, persistence,  
28 proportion of functional CD4<sup>+</sup> T cells, and diversity of EBV antigen specificity. Thus,  
29 our new protocol may pave the way for the next generation of potent unmodified  
30 antigen-specific cell therapies for EBV-associated diseases, including tumors, and  
31 other indications.

32

### 33 INTRODUCTION

34

35 T cell therapies are promising for treatment of hemato-oncological diseases,<sup>1,2</sup> difficult-  
36 to-treat viral infections, and autoimmune diseases.<sup>3,4</sup> The efficacy of these therapies  
37 depends on T cell activation by antigens and *in-vivo* persistence for sustained impact.<sup>5</sup>  
38 Activated T cells can differentiate to stem cell memory (T<sub>SCM</sub>), central memory (T<sub>CM</sub>),  
39 transitional memory (T<sub>TM</sub>) effector memory (T<sub>EM</sub>), and terminally differentiated, short-  
40 lived effector T cells (T<sub>EMRA</sub>).<sup>6</sup> During T cell differentiation, effector functions increase,  
41 but self-renewal capacity declines.<sup>7</sup> The superior proliferation and persistence of T<sub>SCM</sub>  
42 has been demonstrated after adoptive transfer of genetically modified lymphocytes,<sup>8</sup>  
43 chimeric antigen receptor (CAR) T cells, engineered T-cell receptor (TCR)-T cells, and  
44 tumour-infiltrating lymphocytes (TILs).<sup>9,10,11</sup> Long-lasting antigen-specific T<sub>SCM</sub> were  
45 also identified after yellow fever and bacillus Calmette–Guerin (BCG) vaccination.<sup>12,13</sup>  
46 CD8<sup>+</sup> T<sub>SCM</sub> support T-cell responses to chronic LCMV infection<sup>14</sup> and are associated  
47 with improved prognosis in chronic HIV-1 infection.<sup>15</sup>

48

49 T<sub>SCM</sub> might also offer exciting avenues to improve adoptive therapy with virus-specific  
50 T cells (VST) against viral infections that are important causes of morbidity and  
51 mortality of immune-deficient transplant recipients. Adoptive transfer of VST can  
52 restore virus-specific immunity and prevent or cure such viral infections.<sup>16,17</sup> This  
53 includes transfer of EBV-specific cytotoxic T-cell lines (CTLs) that prolongs overall  
54 survival in patients with EBV-driven post-transplant lymphoproliferative disease  
55 (PTLD), other EBV-associated lymphomas and possibly even immunopathologies due  
56 to inefficient EBV specific immune control. However, ~30% of patients show no  
57 response indicating a need for further improvements.<sup>18</sup> Limited long-term response  
58 because of poor persistence and exhaustion of the transferred T cells might contribute  
59 to insufficient response rates. Most clinical studies used VST generated by long-term  
60 expansion with continuous re-stimulation with EBV-antigen expressing lymphoblastoid  
61 cell lines (LCLs),<sup>19</sup> potentially driving the cells to late differentiation stages and  
62 exhaustion.<sup>20</sup> Alternatively, VST can be generated by rapid expansion using a single  
63 stimulation with a viral peptide mixture, but the differentiation state and persistence for  
64 EBV lymphomas is unknown.<sup>21,22</sup>

65

66 Here, we established a novel facile, robust, and clinically applicable protocol for rapid  
67 expansion of EBV-CTLs with a high fraction of EBV-specific T<sub>SCM</sub>. These cells mediate  
68 EBV control *in vitro* and *in vivo* and are superior to previous VST protocols in terms of  
69 tumor infiltration, *in vivo* proliferation, persistence, proportion of functional CD4<sup>+</sup> T  
70 cells, and diversity of EBV antigen specificity.

71

## 72 **RESULTS**

73

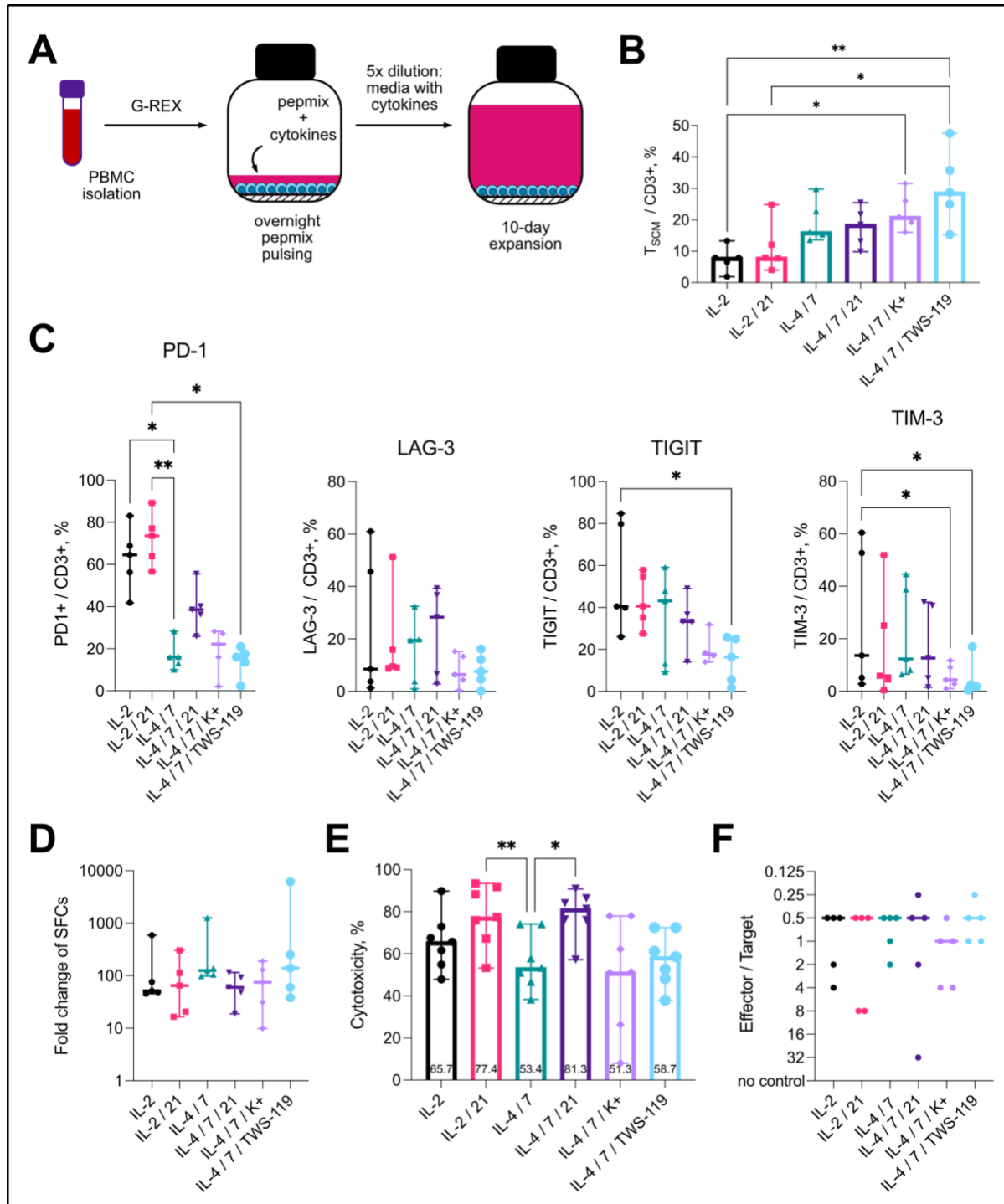
### 74 **Rapid expansion in presence of IL-4 / IL-7 and TWS-119 yields high T<sub>SCM</sub> 75 proportions**

76 To generate EBV-CTLs with high proportions of T<sub>SCM</sub>, we modified the rapid expansion  
77 approach.<sup>21</sup> We stimulated PBMC of healthy EBV-seropositive donors with the EBV  
78 Consensus peptide pool (Figure 1A). We determined the impact of the cytokines IL-7,  
79 IL-15, and IL-21, which promote T cell growth but limit differentiation,<sup>21,23,24</sup> potassium-  
80 rich medium promoting T cell stemness preservation;<sup>25</sup> and the glycogen synthase  
81 kinase-3 $\beta$  (GSK3 $\beta$ ) inhibitor TWS119, which induces Wnt-beta-catenin signaling  
82 limiting cell differentiation and promoting T<sub>SCM</sub> generation.<sup>26</sup> We determined the  
83 proportion of T<sub>SCM</sub> (CD45RA<sup>+</sup> CD45RO<sup>-</sup> CD62L<sup>+</sup> CD27<sup>+</sup>) using flow cytometry  
84 (Supplemental Figure 1A).

85

86 IL-4 / IL-7 promoted T<sub>SCM</sub>, whereas IL-21 had limited impact (Figure 1B). Cytokine  
87 combinations with IL-15 enriched for NK and NKT cells, and the T<sub>SCM</sub> proportions were  
88 insufficient to consider NK cell depletion for the use in the clinical setting  
89 (Supplemental Figure 2A-C). Potassium-rich medium and TWS-119 also promoted  
90 T<sub>SCM</sub>. Overall, IL-4 / IL-7 / TWS-119 yielded the highest T<sub>SCM</sub> proportion (~30%) with  
91 comparable CD4<sup>+</sup> and CD8<sup>+</sup> T cell subsets (Supplemental Figure 1B). This condition  
92 also showed the lowest levels of T cell exhaustion markers (Figure 1C). The different  
93 conditions had limited impact on overall and antigen-specific T cell expansion as  
94 measured by total cell counts, ELISpot assays, and MHC class I multimer staining  
95 (Figure 1D; Supplemental Figure 3A-C). The optimized protocol yielded EBV-CTLs  
96 with reduced short-term cytotoxicity against EBV-lymphoblastoid cell lines (LCLs)  
97 (possibly due to delayed activation of early differentiated T cells) but comparable long-  
98 term LCL control (Figure 1D-E). Thus, rapid expansion in the presence of IL-4, IL-7  
99 and TWS119 yielded EBV-specific CTLs with favorable properties for virus-specific T-

100 cell therapy including high proportion of Tscm, low exhaustion, and efficient long-term  
 101 *in-vitro* cytotoxicity.  
 102



103  
 104 **Figure 1. Establishing rapid Tscm-enriched EBV-CTL ex vivo expansion protocol.** (A) Adapted  
 105 rapid expansion approach. Isolated PBMCs were stimulated with EBV Consensus pepmix in complete  
 106 media. After overnight pulsing, pepmix was diluted 5x with complete media following 10-day incubation.  
 107 (B) Tscm proportions after culturing EBV-CTLs in the presence of different conditions (different cytokine  
 108 combinations, in elevated potassium concentration (K<sup>+</sup>) or with the edition of TWS-119) as detected by

109 flow cytometry; n=5, medians with range. (C) PD-1, LAG-3, TIGIT and TIM-3, exhaustion marker  
110 expression of expanded CTLs; n=5, medians with range. (D) Expansion folds (PBMCs vs. after rapid  
111 expansion) of spot-forming cells after culturing in different conditions; IFN $\gamma$  ELISpot with EBV pepmix  
112 stimulation, n=5, medians with range. (E) Short-term cytotoxicity against autologous EBV-LCLs,  
113 medians with range. (F) Long-term cytotoxicity: 4-week EBV-LCL outgrowth control by expanded T  
114 cells; n=5; medians of controlling E : T were shown. B-F were analyzed by Friedman test,  $\alpha=0.05$ , non-  
115 significant p-values (ns) not shown, \*p < 0.05, \*\*p < 0.005.

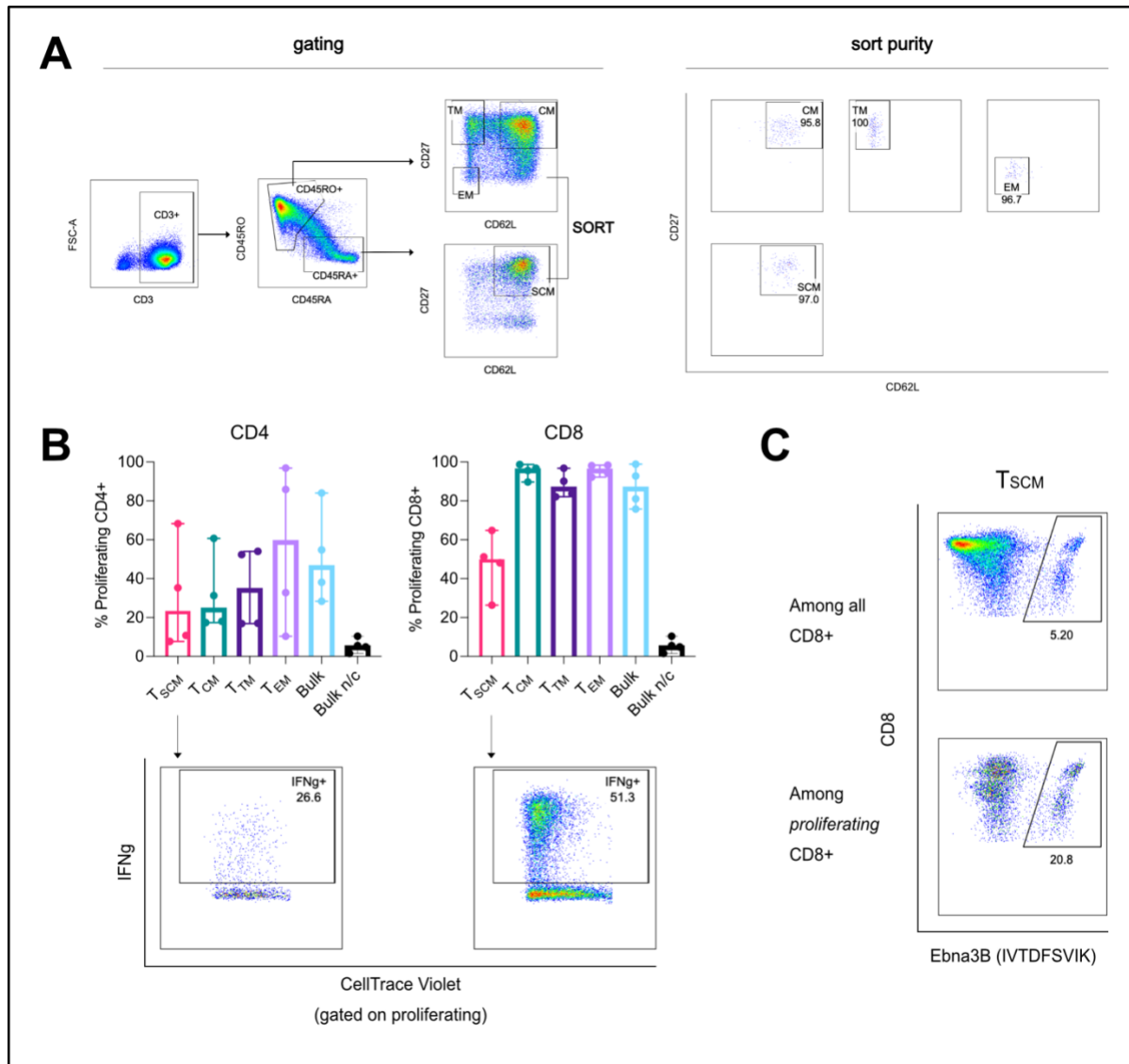
116

## 117 **Expanded TscM are EBV-specific and proliferate in response to restimulation**

118

119 To determine the antigen-specificity of various memory T cell subsets within the  
120 expanded CTLs, we sorted these subsets (Figure 2A) and co-cultured them with  
121 irradiated autologous EBV-transformed LCLs. All memory populations showed  
122 proliferation of CD4 $^{+}$  and particularly CD8 $^{+}$  T cells in these co-cultures (Figure 2B).  
123 IFN $\gamma$  production upon restimulation with EBV peptides confirmed the specificity of  
124 proliferating TscM cells (Figure 2B). This was also consistent with MHC class I multimer  
125 staining (Figure 2C).

126



127

128 **Figure 2. EBV-specific T cells among T<sub>SCM</sub>.** (A) Sorting of different memory population: gating  
129 strategy and representative plots of sort purity. (B) Proliferation of sorted and CTV-stained CD4<sup>+</sup> and  
130 CD8<sup>+</sup> T cell populations after 7-day co-culture of the sorted populations with EBV-LCLs (flow cytometry,  
131 n=4, medians with range) and specificity of proliferating T<sub>SCM</sub> cells (IFNg expression upon re-stimulation  
132 with EBV pepmix, representative plot). (C) Proliferation of specific T<sub>SCM</sub> (stained with a respective MHC  
133 class I multimer, representative plot. Proliferating cells in B-C are cells that proliferated at least once or  
134 more. SCM – stem cell memory, CM – central memory, TM – transitional memory, EM – effector  
135 memory, n/c – no co-culture.

136

### 137 **T<sub>SCM</sub>-enriched EBV-CTLs have a favorable phenotype and broad specificity**

138 The most widely used clinical protocol employs EBV-transformed LCLs as antigen-  
139 presenting cells (APCs) for expanding EBV CTLs in 4-5 week-long co-cultures<sup>18,19</sup>  
140 (CTL-L) (Figure 3A). We compared the established protocol and the newly developed

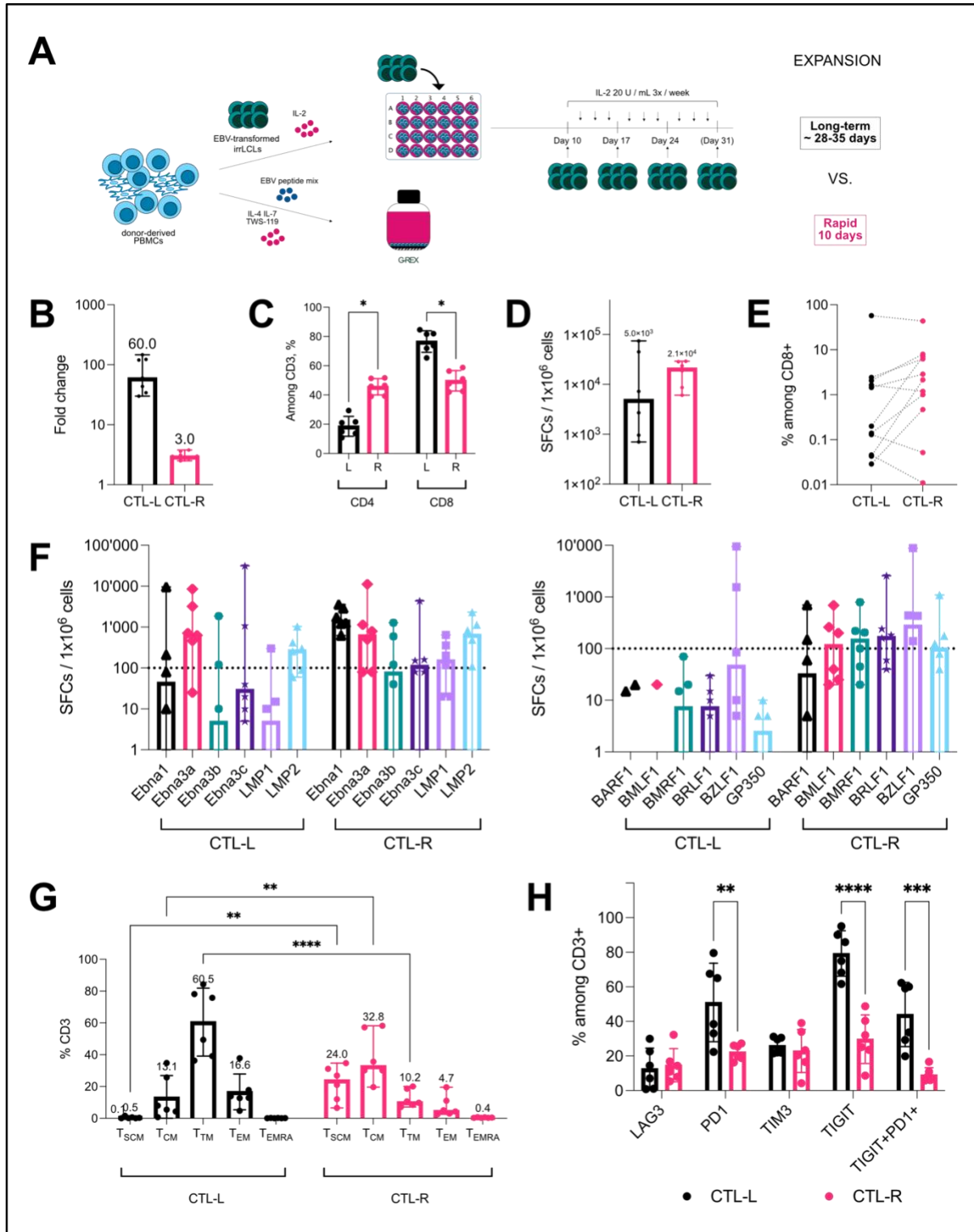
141 T<sub>SCM</sub>-enriching protocol (CTL-R) to evaluate the differences regarding specificity and  
142 phenotypes.

143 CTL-L showed a higher T cell expansion with a lower proportion of CD4<sup>+</sup> T cells than  
144 CTL-R (Figure 3B-C). Overall, EBV specificity was comparable (Figure 3D-E), but  
145 CTL-R had broader antigen specificity for both latent and lytic peptides (Figure 3F).

146 Memory phenotypes differed substantially with higher proportions of earlier  
147 differentiation stages (T<sub>SCM</sub>, T<sub>CM</sub>) in CTL-R and later differentiation stages (T<sub>TM</sub>, T<sub>EM</sub>)  
148 in CTL-L (Figure 3G) and lower levels of exhaustion markers in CTL-R (Figure 3H).

149 Thus, the standard protocol yields more cells, but the novel protocol yields a broader  
150 antigen specificity and more favorable memory and exhaustion phenotypes.

151



152

153 **Figure 3. Comparison of rapidly expanded (CTL-R) and long-term conventionally expanded**  
154 **(CTL-L) EBV-CTLs.** (A) Schematic of two expansion methods. (B) Expansion rates of total cells. n=7,  
155 medians with range. (C) CD4<sup>+</sup> and CD8<sup>+</sup> T cell proportions in expanded cells. 2way ANOVA, n=6,  
156 means with standard deviation (SD). (D) Frequencies of EBV-specific T cells in the expanded products,  
157 IFN $\gamma$  ELISpot after re-stimulation with EBV pepmix; n=6, medians with range, Wilcoxon matched pairs  
158 signed-rank test. (E) Pair-wise comparisons of proportions of different single EBV antigen-specific T  
159 cells measured by respective MHC class I-multimer staining, flow cytometry. n=11, Wilcoxon matched

160 pairs signed-rank test. (F) Frequencies of single protein-specific T cells in the expanded products (latent  
161 – left graph, lytic – right graph), IFN $\gamma$  ELISpot after re-stimulation with peptide pools derived from single  
162 EBV proteins, the dotted line indicates the threshold (spot calculations below the line were considered  
163 not significantly different from control). n=6, medians with range, Wilcoxon matched pairs signed-rank  
164 test. (G) Memory phenotypes and (H) exhaustion marker expression, flow cytometry. n=6, means with  
165 SD, 2way ANOVA. For C-H:  $\alpha=0.05$ , non-significant p-values (ns) not shown, p < 0.05, \*\*p < 0.005, \*\*\*p  
166 < 0.001, \*\*\*\*p < 0.0001.

167

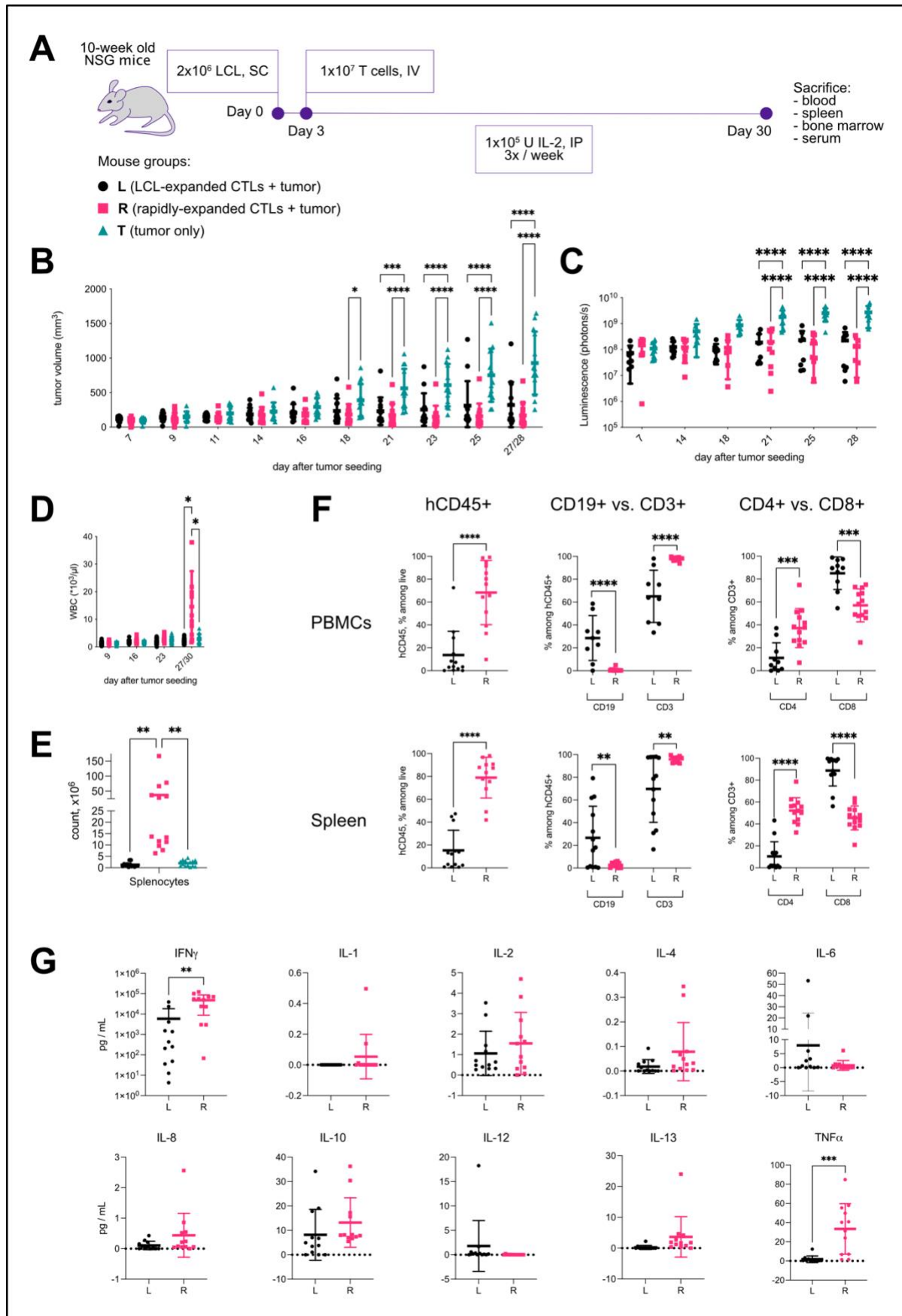
## 168 **T<sub>SCM</sub>-enriched EBV-CTLs control tumor growth, proliferate, persist and release 169 pro-inflammatory cytokines *in vivo***

170 To test the *in-vivo* function of T<sub>SCM</sub>-enriched EBV-CTL, we used a well-characterized  
171 mouse model of EBV-driven post-transplant lymphoproliferative disease (PTLD).<sup>27,28</sup>  
172 2x10<sup>6</sup> luciferase-expressing EBV-LCLs were injected subcutaneously followed by  
173 adoptive transfer of 1x10<sup>7</sup> autologous CTL-L or CTL-R three days later i.v. into NOD-  
174 scid gamma<sub>c</sub><sup>-/-</sup> (NSG) mice supplemented with high doses of human IL-2 to support T  
175 cells in the NSG system (Figure 4A). Tumor growth dynamics revealed that both CTL-  
176 L and CTL-R controlled tumor growth equally well over four weeks (Figure 4B-C).  
177 Three out of 13 mice (23%) receiving CTL-R but no mice receiving CTL-L lost weight  
178 at late time points (supplemental Figure 5) together with increased levels of white  
179 blood cells (WBCs) and higher serum IFN $\gamma$  and TNF $\alpha$  levels in the CTL-R group  
180 (Figure 4D,G). Spleen weights and splenocyte counts were also higher for CTL-R than  
181 CTL-L and tumor-only groups (Figure 4E, supplemental Figure 4A) and spleen,  
182 peripheral blood and bone marrow contained more human CD45<sup>+</sup> (hCD45<sup>+</sup>) cells.  
183 Most of these cells were CD3<sup>+</sup> indicating substantial *in-vivo* expansion of T cells  
184 (Figure 4F, supplemental Figure 4B). CD8<sup>+</sup> T cells expanded initially more in mice  
185 receiving CTL-R but CD8<sup>+</sup>/CD4<sup>+</sup> T cell ratios returned to pre-infusion levels at later  
186 time points, whereas CD8<sup>+</sup> T cells dominated throughout in mice receiving CTL-L  
187 group (Figure 4F, supplemental Figure 4C).

188

189 Thus, both long-term and rapidly expanded EBV CTLs efficiently control tumor growth,  
190 but T<sub>SCM</sub>-enriched CTLs generate more CD4<sup>+</sup> and CD8<sup>+</sup> T cells and persist better *in*  
191 *vivo*.

192



193

194 **Figure 4. Expansion of CTL-R *in vivo*.** (A) Schematic of the *in vivo* experiments. 2x10<sup>6</sup> tumor cells  
 195 (luciferase-expressing EBV-LCLs) / mouse were injected into NSG mice subcutaneously, and on day 3

196  $1 \times 10^7$  autologous long-term or rapidly expanded EBV-CTLs per mouse were infused intravenously.  
197 Groups of tumor-only mice were kept as a negative control. All mice were supplemented with  $1 \times 10^5$  U  
198 / hIL-2 3x / week. Mice were sacrificed after ~4 weeks and organs were collected. Pooled data from  
199 three independent experiments with 3 different donors (n = 13 mice/group) is shown in further plots  
200 unless there was no sample available. Data from CTL-L-injected mice marked in black circles, CTL-R  
201 – in pink squares, and tumor-only mice – in green-blue triangles. Tumor growth dynamic measured by  
202 caliper –  $\sim 3x$  / week (B) and tumor luminescence measured 1-2x / week (C). (D) *In vivo* white blood  
203 cell (WBC) expansion dynamic, flow cytometry of weekly bleedings. (E) Splenocyte total counts after  
204 sacrifice. (F) Proportions of human CD45 $^+$  cells, CD3 $^+$  and CD19 $^+$  among human CD45 $^+$  cells, and CD4 $^+$   
205 and CD8 $^+$  among human CD3 $^+$  in peripheral blood (PBMC) and spleen, flow cytometry. (G) Multiplex  
206 analysis of human cytokines in the murine sera collected after sacrifice. For B-F, means with SD; mixed-  
207 effects analysis (B-D, G), 1-way ANOVA and Tukey's multiple comparrisos test (E) and multiple  
208 unpaired t test (F),  $\alpha=0.05$ , non-significant p-values not shown, p < 0.05, \*\*p < 0.005, \*\*\*p < 0.001, \*\*\*\*p  
209 < 0.0001.

210

### 211 **T<sub>scm</sub>-enriched EBV CTLs infiltrate tumors and have broad antigen specificity**

212 To determine the specificity of EBV-CTLs expanded *in vivo*, we measured tumor  
213 infiltration of CD8 $^+$  T cells by immunohistochemistry (Figure 5A-B). However, flow  
214 cytometry revealed a significantly higher CD3 $^+$  T cell infiltration and particularly a  
215 higher infiltration of CD4 $^+$  T cells into tumors of mice receiving transfer of CTL-R  
216 compared to CTL-L (Figure 5C-D).

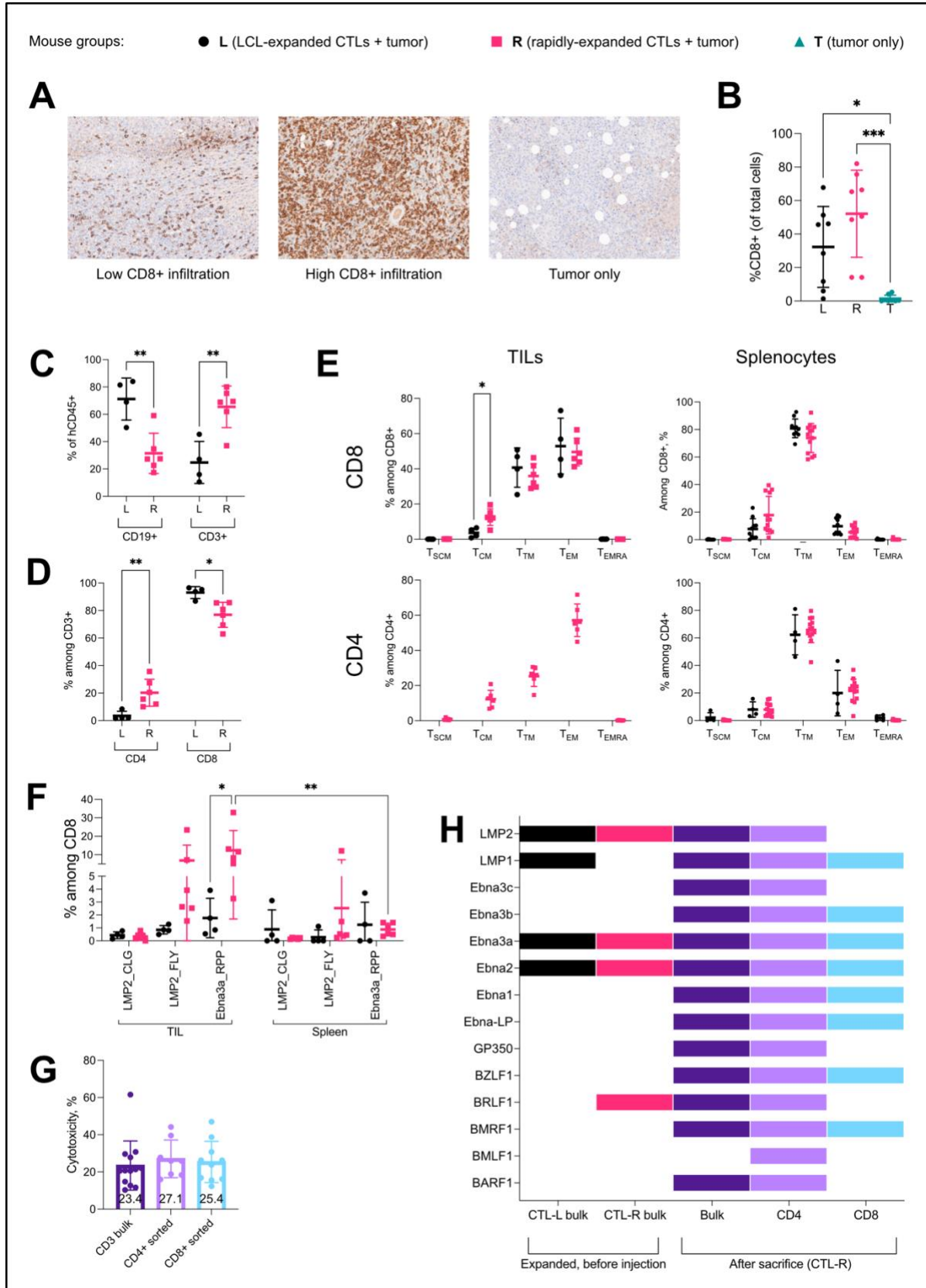
217

218 CTL-R-derived tumor-infiltrating lymphocytes (TILs) showed a less differentiated  
219 phenotype with more T<sub>CM</sub> compared to CTL-L (Figure 5E), although T<sub>scm</sub> TILs were  
220 rare in both groups. Tumor-infiltrating T cells of both groups were more differentiated  
221 with a predominance of T<sub>EM</sub> compared to T cells not derived from tumors, with high  
222 proportions of T<sub>TM</sub> in spleen and other organs (Figure 5E, Supplemental Figure 6A-C).  
223 A higher proportion of CTL-R-derived antigen-specific TILs was detected via specific  
224 EBV peptide loaded MHC class I multimers compared to the CTL-L group and CD8 $^+$   
225 T cells in spleen from both groups (Figure 5F).

226

227 Both CD4 $^+$  and CD8 $^+$  splenocytes derived from CTL-R showed short-term *in-vitro*  
228 cytotoxicity against EBV-LCLs (there was insufficient expansion in the CTL-L group to  
229 perform similar experiments) (Figure 5G). ELISpot assays with peptides from 14  
230 different EBV proteins revealed a remarkable increase of antigen coverage in CTL-R  
231 derived splenocytes and particularly CD4 $^+$  T cells (Figure 5H). Thus, transferred EBV-

232 specific Tscm-enriched CTLs (CTL-R) showed robust proliferation and longevity, and  
 233 reconstituted a wide antigen diversity of different T cell compartments.  
 234



235

236 **Figure 5. Specificity of expanding EBV-CTLs *in vivo*.** Immunohistochemistry analysis of CD8<sup>+</sup> tumor  
237 infiltrating lymphocytes: (A) representative pictures of samples with low and high CD8<sup>+</sup> T cell infiltration  
238 as well as tumor only, CD8<sup>+</sup> cells are stained in brown, nuclei – in blue; (B) proportions of tumor  
239 infiltrating CD8<sup>+</sup> lymphocytes by treatment group (pooled data from available samples from two  
240 experiments, 10 mice / group). (C) Proportions of CD3<sup>+</sup> vs. CD19<sup>+</sup> among human CD45<sup>+</sup> cells in TILs,  
241 and (D) proportions of CD4<sup>+</sup> vs. CD8<sup>+</sup> among CD3<sup>+</sup> T cells, measured by flow cytometry. (E) A shift of  
242 CD8<sup>+</sup> and CD4<sup>+</sup> T cell memory phenotypes in TILs vs. spleen (pooled data of available samples). (F)  
243 Proportions of EBV-specific MHC class I-multimer-stained CD8<sup>+</sup> T cells. (G) *in vitro* short-term  
244 cytotoxicity of bulk, separated CD4<sup>+</sup> and CD8<sup>+</sup> splenocytes against autologous LCLs (pooled data from  
245 all available samples). (H) Presence of specific response of bulk CTL-L and CTL-R cultures before  
246 injection vs CTL-R bulk, CD4<sup>+</sup> and CD8<sup>+</sup> splenocytes after sacrifice to stimulation with single-EBV  
247 protein antigen pools measured by ELISpot (based on mean data from all available samples collected  
248 from one experiment / one donor). For B-G, means with SD; 1-way ANOVA and Tukey's multiple  
249 comparrisos test (B, G); multiple unpaired t test (C-E) and 2way ANOVA (F) were used.

250

## 251 **DISCUSSION**

252

253 Adoptive T cell therapy (ACT) therapeutically transfers specifc T cell immunity to  
254 patients. Persistence of memory T cell subsets in the recipients is often critical for  
255 long-term efficacy, but difficult to attain. Very early differentiated T<sub>SCM</sub> cells,  
256 characterized by high self-renewal, engraftment and persistence, can reconstitute all  
257 types of effector and memory T cell subsets<sup>29</sup> and show encouraging results in T cell  
258 therapy.<sup>8,10,11</sup>

259

260 T<sub>SCM</sub> might be also a promising avenue for treatment of viral infections such as EBV  
261 in transplant patients. Anti-viral ACT is an active field with several ongoing phase III  
262 trials (clinicaltrials.gov: NCT03394365, NCT04832607, NCT04832607,  
263 NCT04832607). However, current strategies are still suboptimal with response rates  
264 of only around 70% for most viruses.<sup>18</sup> To test T<sub>SCM</sub> for ACT against EBV infections, T  
265 cell priming and several steps of cell sorting can be used, but the complexity of this  
266 method makes it difficult to translate to the clinical setting.<sup>30</sup> Moreover, CD4<sup>+</sup> T cells  
267 are depleted which might impair sustaining adoptive immunity.<sup>31</sup>

268

269 Here, we developed a novel method to enrich both CD4<sup>+</sup> and CD8<sup>+</sup> T<sub>SCM</sub> EBV-CTL  
270 from PBMCs with minimal cell handling steps. We did not use the common stimulation  
271 with autologous EBV-LCLs,<sup>32</sup> which requires 4 to 8 weeks and yields predominantly

272 late-stage  $T_{EM}$ .<sup>33,34</sup> Continuous re-stimulation of T cells can promote T cell  
273 exhaustion<sup>20</sup> defined as a reduced functional capacity.<sup>35</sup> Instead, we adapted a rapid  
274 expansion protocol that is safe and effective in transplant patients<sup>36</sup> and yields a higher  
275 proportion of  $T_{CM}$ , which are superior to  $T_{EM}$  in antiviral activity and persistence.<sup>37,38</sup>  
276 Due to its minimal cell handling steps, this protocol can be easily transferred to the  
277 clinic. The overall yield is lower than for long-term stimulation, but this is not a limiting  
278 factor because sufficient starting numbers of PBMCs can be obtained with standard  
279 blood donations.

280

281 We systematically tested various cytokines and other conditions to maximize the  
282 proportion of  $T_{SCM}$  and discovered that a combination of IL-4 and IL-7 with induction  
283 of the Wnt/β-catenin pathway using TWS119 triggered efficient enrichment of EBV-  
284 specific  $T_{SCM}$  with broad coverage of antigens including lytic antigens. T cells specific  
285 for lytic antigens can be relevant for treatment of diseases like nasopharyngeal  
286 carcinoma (NPC) in a therapeutic setting<sup>39,40</sup> as well as prophylaxis of EBV-associated  
287 B cell malignancies and NPC, as the lytic phase of EBV contributes to oncogenesis.<sup>41-</sup>  
288<sup>43</sup> T cells specific for lytic antigens are difficult to obtain with long-term stimulation  
289 using EBV-LCLs which exhibit latency III and express predominantly latent EBV  
290 antigens.<sup>44</sup> A wide diversity of antigen specificity also broadens the scope of cell  
291 therapy and reduces the risk of relapse due to antigen escape.<sup>45</sup> Moreover, lytic EBV  
292 antigen-specific CD8<sup>+</sup> T cells require early memory differentiation with maintained  
293 CD27 expression for their protective function,<sup>46</sup> and this is ensured by our rapid  
294 expansion protocol.

295

296 A key aspect of an ACT product is the balance between CD4<sup>+</sup> and CD8<sup>+</sup> T cell  
297 populations,<sup>47,48</sup> and a high CD4<sup>+</sup> T cell proportion is associated with better responses  
298 to anti-EBV ACT for treatment of PTLD.<sup>49</sup> In contrast to the widely used long-term  
299 stimulation with low yields of CD4<sup>+</sup> T cells, our novel protocol enriched CD4<sup>+</sup> and CD8<sup>+</sup>  
300 EBV-specific T cells in all memory populations. The high CD4<sup>+</sup> T cell proportion was  
301 maintained after adoptive transfer and was reflected in tumor infiltration, and CD4<sup>+</sup> T  
302 cells recovered a broad antigen-specific profile *in vivo*. These EBV-specific CD4<sup>+</sup> T  
303 cells may contribute to control of various EBV diseases.

304

305 Limitations of this study include lack of long-term data beyond 4 weeks in mice. High  
306 human T-cell engraftment in murine organs may lead to xeno-GVHD,<sup>50</sup> signs of which  
307 (e.g., weight loss) were observed in some mice in the CTL-R group. Nevertheless, the  
308 efficient CTL-R infiltration into tumors, the *in vitro* cytotoxicity and the specific  
309 responses of splenocytes indicated high specificity of the expanded T cells. Moreover,  
310 this mouse model-related aspect may not be indicative of potential issues in a clinical  
311 application because rapidly expanded virus-specific T cells are safe upon the adoptive  
312 transfer into patients.<sup>22</sup>

313

314 In conclusion, we demonstrate that our novel protocol yields promising EBV-specific  
315 T<sub>SCM</sub>-enriched CTLs with favorable properties for VST production, such as early  
316 differentiated memory composition, low exhaustion, high tumor infiltration, efficient  
317 CD4<sup>+</sup> and CD8<sup>+</sup> T cell mediated cytotoxicity, long-term persistence, and broad antigen  
318 specificity. This may pave the way for the next generation of unmodified antigen-  
319 specific cell therapies against viral infections. The safety and efficacy as well as the  
320 clonal diversity of these VST remain to be investigated in an upcoming clinical trial.

321

## 322 METHODS

323

### 324 Peptides

325 The PepTivator EBV Consensus peptide pool (Miltenyi Biotec), and single peptide  
326 pools from various EBV antigens (latent: EBNA-LP, EBNA2, EBNA3a, EBNA3b,  
327 EBNA3c, LMP1; lytic: BARF1, BMLF1, BMRF1, BRLF1, BZLF1, GP350/GP340) (JPT  
328 Peptide Technologies) were used for T cell stimulation.

329

330 *Blood donors, cell culture and generation and expansion of EBV-specific T-cell lines*  
331 Blood was obtained after informed consent from healthy donors in accordance with  
332 the Declaration of Helsinki. The study was approved by the local ethic committee  
333 (Ethikkommission Nordwest- und Zentralschweiz, Project ID PB\_2018-00081).  
334 Donors were typed for HLA class I and class II alleles. Human peripheral blood  
335 mononuclear cells (PBMCs) were isolated from EDTA blood of healthy donors and <sup>51</sup>  
336 EBV-transformed lymphoblastoid cell lines (LCL) were generated and cultured in  
337 LCM-10 media according to previously published protocols<sup>52</sup> (Supplemental  
338 Materials). Long-term EBV-CTL expansion with LCL re-stimulations and rapid

339 expansion protocols were adapted from previously described protocols.<sup>19 21</sup> All T cells  
340 were expanded in CTL-M (Supplemental methods). For rapid expansion, PBMCs were  
341 cultured in a G-Rex bioreactor (Wilson&Wolf). 3x10<sup>6</sup> PBMCs / well of a 24-well G-Rex  
342 plate or 1.5x10<sup>7</sup> / well of a 6-well G-Rex plate were cultured. On day 0, cells were  
343 pulsed overnight in CTL-M (or CTL-M with high K<sup>+</sup> when applicable) containing the  
344 EBV Consensus peptide pool (pepmix) and supplemented with cytokines (and TWS-  
345 119 when applicable). Afterwards the pepmix (and TWS-119 if applicable) was diluted  
346 5x with CTL-M supplemented only with cytokines. Cell culture went on up to day 10-  
347 12 without further supplementation.

348 For long-term EBV-CTL expansion, PBMCs were stimulated with autologous EBV-  
349 LCLs at effector : target (E:T) = 40:1 for 10 days (2x10<sup>6</sup> PBMCs/well of a 24-well cell  
350 culture plate) without cytokine supplementation. Afterwards T cells were re-stimulated  
351 weekly at E:T=4:1) and supplemented with 20 U/mL IL-2 3x / week until day 28-35.<sup>19</sup>  
352 LCL culture is described in Supplemental Methods.

353

#### 354 *EBV-LCL generation and culture*

355 PBMCs were incubated with recombinant B95-8 or B95-8-fLuc EBV strains (both gifts  
356 from Dr. Wolfgang Hammerschmidt, Helmholtz Center Munich, Germany), cultured in  
357 LCM-10 media and were treated with 2 µg/ml Cyclosporin A (Sigma Aldrich) and 2  
358 µg/ml CpG ODN 2006 (InvivoGen) weekly until the transformation. Non-irradiated  
359 LCLs were always cultured in LCM-10 media (including cytotoxicity and outgrowth  
360 assays).

361

#### 362 *Co-culture with autologous EBV-LCLs*

363 After fluorescence-assisted cell sorting (FACS) (staining described below), sorted  
364 cells were recovered for 3 days in CTL-M supplemented with IL-4 and IL-7. Afterwards,  
365 autologous LCLs were irradiated and T cells were stained with CellTrace Violet (CTV).  
366 Irradiated LCLs were cultured with T cells at a ratio 1:1 for one week. Then cells were  
367 harvested and analyzed by flow cytometry (see below).

368

#### 369 *Short-term and long-term in-vitro cytotoxicity*

370 Short-term 6-hour killing assay and long-term 4-week outgrowth assay were adopted  
371 as previously published<sup>53</sup>. Briefly, for killing assay, EBV-CTLs were incubated with

372 target EBV-LCLs at an effector (E) to target (T) ratio = 30:1 for 6 h. Afterwards, cells  
373 were stained for viability (Zombie Aqua), apoptosis (CellEvent Blue), CD3 and CD19  
374 surface markers (see the panels below). Cytotoxicity was calculated according to the  
375 following formula:  $100 - ([V_{\text{test}} / V_{\text{control}}] * 100)$  where  $V$  = % viable (CellEvent<sup>+</sup> Zombie  
376 Aqua<sup>-</sup>) CD19<sup>+</sup> cells.

377 For outgrowth assay (long-term cytotoxicity assay), T cells were incubated with EBV-  
378 LCLs at different effector / target ratios in triplicates for 4 weeks. The readout was the  
379 lowest E/T ratio controlling the outgrowth of LCLs which was determined  
380 microscopically and confirmed by flow cytometry.

381

382 *IFNy ELISpot, intracellular cytokine staining and V-PLEX*

383 EBV-responsive T cells were identified by stimulation with EBV peptides. Enzyme-  
384 linked immunospot assay (ELISpot)<sup>53</sup> and intracellular cytokine (ICC) staining for flow  
385 cytometry detection<sup>54</sup> were done as previously published.

386 Human cytokine presence in murine blood sera was analyzed using V-PLEX human  
387 pro-inflammatory panel-1 and detected by Mesoscale system according to  
388 manufacturer's instructions.

389

390 *Immunomagnetic cell sorting*

391 CD4<sup>+</sup> and CD8<sup>+</sup> T cells were isolated using the MACS CD4<sup>+</sup> / CD8<sup>+</sup> isolation kit  
392 (Miltenyi Biotec) according to the manufacturer's instructions.

393

394 *Immunohistochemistry*

395 Tumors were fixed in a 4% paraformaldehyde solution; further sample preparation and  
396 immunohistochemistry staining were done commercially by the Pathology Department  
397 of the University Hospital of Basel. Slides were acquired on an automated slide  
398 scanning brightfield microscope (Vectra) and positive cells were quantified using  
399 inForm automated image analysis software (Akoya Biosciences).

400

401 *Flow cytometry and FACS-based cell sorting*

402 All flow cytometry panels are described in detail in the supplemental materials.  
403 If applicable, red blood cells were lysed using ACK (Ammonium-Chloride-Potassium)  
404 lysis buffer until the pellet appeared no longer red. If applicable, whole-cell staining for  
405 proliferation tracing and viability staining were performed in PBS according to

406 manufacturer's instructions. Surface staining with antibodies and MHC class I-  
407 multimers (if applicable) was performed in FACS buffer (5% FBS, 0.1% NaN3 in PBS).  
408 For intracellular staining, cells were fixed with fixation buffer (Biolegend, 420801) and  
409 stained for intracellular markers in the permeabilization buffer (Biolegend, 421002)  
410 according to manufacturer's instructions. For combined intracellular/intranuclear  
411 staining, cells were fixed and permeabilized using Transcription-Factor Buffer Set (BD,  
412 #562574) according to the manufacturer's instructions.

413 Spectral flow cytometry was performed on Cytek Aurora. Fluorescence-assisted cell  
414 sorting was performed with BD FACSMelody. Weekly bleedings of mice were  
415 analysed with BD LSRFortessa. Data were analyzed using FlowJo software.  
416 FlowSOM algorithm was used to define memory T cell populations: stem cell memory  
417 ( $T_{SCM}$ ) as  $CD45RA^+CD45RO^-CD62L^+CD27^+$ , central memory ( $T_{CM}$ ) as  $CD45RA^-$   
418  $CD45RO^+CD62L^+CD27^+$ , transitional memory  $T_{TM}$  as  $CD45RA^-CD45RO^+CD62L^-$   
419  $CD27^+$ , effector memory  $T_{EM}$  as  $CD45RA^-CD45RO^+CD62L^-CD27^-$ , and terminally  
420 differentiated  $T_{EMRA}$  as  $CD45RA^+CD45RO^-CD62L^-CD27^-$ .

421

#### 422 *Procedures in vivo*

423 Animal experiments were conducted according to the licence approved by the  
424 veterinary office of the canton of Zurich, Switzerland (ZH049/20). NSG (NOD.Cg-  
425 *Prkdc*<sup>scid</sup> *Il2rg*<sup>tm1Wjl</sup>/SzJ (#005557)) or NSG-A2 (NOD.Cg-*Mcphe1*<sup>Tg(HLA-A2.1)1Eng</sup> *Prkdc*<sup>scid</sup>  
426 *Il2rg*<sup>tm1Wjl</sup>/SzJ (#009617)) mice were purchased from The Jackson Laboratory and  
427 bred and housed under specific pathogen-free conditions at the Laboratory Animal  
428 Services Center (LASC) of the University of Zurich. Experiments were initiated at 6-  
429 12 weeks of age. The mouse models were adapted from previous studies<sup>27,28</sup>. LCL  
430 tumor cells were injected subcutaneously into the left flank under isoflurane narcosis.  
431  $2 \times 10^6$  tumor cells were resuspended in PBS and right before injection mixed in a 1:1  
432 V/V ratio with Corning® Matrigel® Growth Factor Reduced (GFR) Basement  
433 Membrane Matrix. Three days after tumor injection,  $1 \times 10^7$  T cells were adoptively  
434 transferred by tail vein injection. T cell expansion was supported by i.p. injection of  $10^5$   
435 IU recombinant human IL-2 (3x/week, Peprotech), or as stated otherwise. Tumor size  
436 was monitored by caliper (3x/week) and bioluminescent imaging for tumor cells  
437 transformed with a luciferase encoding recombinant EBV strain (generous gift of Dr.  
438 Wolfgang Hammerschmidt, Helmholtz Institute Munich, Germany; 2x/week). General  
439 health was monitored by weighing and health parameter scoring 3x/week or daily,

440 according to the animal license. Peripheral blood composition and expansion of  
441 adoptively transferred T cells were monitored by weekly tail vein bleeding and flow  
442 cytometric analysis (Supplementary Materials) on BD Fortessa. White blood cell  
443 counts were determined from full blood with an automatic cell counter (DxH 500,  
444 Beckman Coulter). For bioluminescent imaging, mice were injected with 5 $\mu$ l/g body  
445 weight of 15mg/ml VivoGlo™ Luciferin (Promega) and imaged 10 minutes after  
446 injection in an IVIS machine (PerkinElmer) under isoflurane narcosis. Animals were  
447 euthanized when they met pre-defined criteria stated in the animal license, or when  
448 the control group met the end-point criteria.

449

450 *Statistics*

451 Analyses were conducted using Prism software (GraphPad). Data of individual donors  
452 are shown as representative experiments or medians with standard deviations (SD).  
453 Combined data of different donors are given as median with range.

454

455 *Data Sharing Statement*

456 For original data, please contact nina.khanna@usb.ch.

457

458 **Acknowledgements**

459

460 We would like to thank the FACS Core facility of the Department of Biomedicine,  
461 University Hospital of Basel, FACS Core facility and Animal Facility of the Institute of  
462 Experimental Immunology, University of Zurich, for excellent support. We thank Joëlle  
463 Handschin for the assistance in the multiplex assay and Prof. Dr. Dirk Bumann for the  
464 valuable scientific and writing advice. Big thanks go to all the blood donors participated  
465 in the study. This work was supported by Cancer Research Switzerland Grant No.  
466 KFS-4371-02-2018 and KFS-5292-02-2021 (to O.C.), the Swiss National Foundation  
467 Grant 32003B\_204944 (to N.K.), NCCR Antiresist Grant No. 180541, Switzerland (to  
468 N.K.), Bangerter–Rhyner Stiftung (to N.K.).

469

470 **Authorship contributions**

471

472 DP, CS and NK designed the study. DP, CS and BA performed *in vitro* experiments  
473 and analysis; GB assisted with the EBV-LCL transformation. DP, JM, OC, CM and NK  
474 designed *in vivo* experiments; OC and CM supervised *in vivo* experiments; DP and  
475 JM performed *in vivo* experiments and analysis; DP and NK wrote the manuscript.

476

477 **Disclosure of Conflicts of Interest**

478

479 The authors declare no conflicts of interest.

480

481 **REFERENCES**

482

- 483 1. Maus MV, Fraietta JA, Levine BL, Kalos M, Zhao Y, June CH. Adoptive  
484 immunotherapy for cancer or viruses. *Annu Rev Immunol*. 2014;32:189-225.
- 485 2. Rosenberg SA, Restifo NP. Adoptive cell transfer as personalized  
486 immunotherapy for human cancer. *Science*. 2015;348(6230):62-68.
- 487 3. Barrett AJ, Prockop S, Bolland CM. Virus-Specific T Cells: Broadening  
488 Applicability. *Biol Blood Marrow Transplant*. 2018;24(1):13-18.
- 489 4. Scott DW. Genetic Engineering of T Cells for Immune Tolerance. *Mol Ther*  
490 *Methods Clin Dev*. 2020;16:103-107.
- 491 5. Redeker A, Arens R. Improving Adoptive T Cell Therapy: The Particular Role  
492 of T Cell Costimulation, Cytokines, and Post-Transfer Vaccination. *Front*  
493 *Immunol*. 2016;7:345.

494 6. Mahnke YD, Brodie TM, Sallusto F, Roederer M, Lugli E. The who's who of T-  
495 cell differentiation: human memory T-cell subsets. *Eur J Immunol*.  
496 2013;43(11):2797-2809.

497 7. Joshi NS, Kaech SM. Effector CD8 T cell development: a balancing act  
498 between memory cell potential and terminal differentiation. *J Immunol*.  
499 2008;180(3):1309-1315.

500 8. Oliveira G, Ruggiero E, Stanghellini MT, et al. Tracking genetically engineered  
501 lymphocytes long-term reveals the dynamics of T cell immunological memory.  
502 *Sci Transl Med*. 2015;7(317):317ra198.

503 9. Wang F, Cheng F, Zheng F. Stem cell like memory T cells: A new paradigm in  
504 cancer immunotherapy. *Clin Immunol*. 2022;241:109078.

505 10. Fraietta JA, Lacey SF, Orlando EJ, et al. Determinants of response and  
506 resistance to CD19 chimeric antigen receptor (CAR) T cell therapy of chronic  
507 lymphocytic leukemia. *Nat Med*. 2018;24(5):563-571.

508 11. Biasco L, Izotova N, Rivat C, et al. Clonal expansion of T memory stem cells  
509 determines early anti-leukemic responses and long-term CAR T cell  
510 persistence in patients. *Nat Cancer*. 2021;2(6):629-642.

511 12. Fuertes Marraco SA, Soneson C, Cagnon L, et al. Long-lasting stem cell-like  
512 memory CD8+ T cells with a naive-like profile upon yellow fever vaccination.  
513 *Sci Transl Med*. 2015;7(282):282ra248.

514 13. Mpande CAM, Dintwe OB, Musvosvi M, et al. Functional, Antigen-Specific  
515 Stem Cell Memory (TSCM) CD4(+) T Cells Are Induced by Human  
516 Mycobacterium tuberculosis Infection. *Front Immunol*. 2018;9:324.

517 14. Utzschneider DT, Charmoy M, Chennupati V, et al. T Cell Factor 1-  
518 Expressing Memory-like CD8(+) T Cells Sustain the Immune Response to  
519 Chronic Viral Infections. *Immunity*. 2016;45(2):415-427.

520 15. Ribeiro SP, Milush JM, Cunha-Neto E, et al. The CD8(+) memory stem T cell  
521 (T(SCM)) subset is associated with improved prognosis in chronic HIV-1  
522 infection. *J Virol*. 2014;88(23):13836-13844.

523 16. Houghtelin A, Bolland CM. Virus-Specific T Cells for the Immunocompromised  
524 Patient. *Front Immunol*. 2017;8:1272.

525 17. Heslop HE, Sharma S, Rooney CM. Adoptive T-Cell Therapy for Epstein-Barr  
526 Virus-Related Lymphomas. *J Clin Oncol*. 2021;39(5):514-524.

527 18. Walti CS, Stuehler C, Palianina D, Khanna N. Immunocompromised host  
528 section: Adoptive T-cell therapy for dsDNA viruses in allogeneic  
529 hematopoietic cell transplant recipients. *Curr Opin Infect Dis*. 2022;35(4):302-  
530 311.

531 19. Rooney CM, Smith CA, Ng CY, et al. Infusion of cytotoxic T cells for the  
532 prevention and treatment of Epstein-Barr virus-induced lymphoma in  
533 allogeneic transplant recipients. *Blood*. 1998;92(5):1549-1555.

534 20. Zou D, Dai Y, Zhang X, et al. T cell exhaustion is associated with antigen  
535 abundance and promotes transplant acceptance. *Am J Transplant*.  
536 2020;20(9):2540-2550.

537 21. Gerdemann U, Keirnan JM, Katari UL, et al. Rapidly generated multivirus-  
538 specific cytotoxic T lymphocytes for the prophylaxis and treatment of viral  
539 infections. *Mol Ther*. 2012;20(8):1622-1632.

540 22. Gerdemann U, Katari UL, Papadopoulou A, et al. Safety and clinical efficacy  
541 of rapidly-generated trivirus-directed T cells as treatment for adenovirus, EBV,  
542 and CMV infections after allogeneic hematopoietic stem cell transplant. *Mol*  
543 *Ther*. 2013;21(11):2113-2121.

544 23. Pethe K, Sequeira PC, Agarwalla S, et al. A chemical genetic screen in  
545 Mycobacterium tuberculosis identifies carbon-source-dependent growth  
546 inhibitors devoid of in vivo efficacy. *Nat Commun.* 2010;1(57):57.

547 24. Khalaf WS, Garg M, Mohamed YS, Stover CM, Browning MJ. In vitro  
548 Generation of Cytotoxic T Cells With Potential for Adoptive Tumor  
549 Immunotherapy of Multiple Myeloma. *Front Immunol.* 2019;10:1792.

550 25. Vodnala SK, Eil R, Kishton RJ, et al. T cell stemness and dysfunction in  
551 tumors are triggered by a common mechanism. *Science.* 2019;363(6434).

552 26. Gattinoni L, Zhong XS, Palmer DC, et al. Wnt signaling arrests effector T cell  
553 differentiation and generates CD8+ memory stem cells. *Nat Med.*  
554 2009;15(7):808-813.

555 27. Koehne G, Doubrovin M, Doubrovina E, et al. Serial in vivo imaging of the  
556 targeted migration of human HSV-TK-transduced antigen-specific  
557 lymphocytes. *Nat Biotechnol.* 2003;21(4):405-413.

558 28. Hiwarkar P, Qasim W, Ricciardelli I, et al. Cord blood T cells mediate  
559 enhanced antitumor effects compared with adult peripheral blood T cells.  
560 *Blood.* 2015;126(26):2882-2891.

561 29. Gattinoni L, Restifo NP. Moving T memory stem cells to the clinic. *Blood.*  
562 2013;121(4):567-568.

563 30. Kondo T, Imura Y, Chikuma S, et al. Generation and application of human  
564 induced-stem cell memory T cells for adoptive immunotherapy. *Cancer Sci.*  
565 2018;109(7):2130-2140.

566 31. Li K, Donaldson B, Young V, et al. Adoptive cell therapy with CD4(+) T helper  
567 1 cells and CD8(+) cytotoxic T cells enhances complete rejection of an  
568 established tumour, leading to generation of endogenous memory responses  
569 to non-targeted tumour epitopes. *Clin Transl Immunology.* 2017;6(10):e160.

570 32. Prockop S, Doubrovina E, Suser S, et al. Off-the-shelf EBV-specific T cell  
571 immunotherapy for rituximab-refractory EBV-associated lymphoma following  
572 transplant. *J Clin Invest.* 2019.

573 33. Ricciardelli I, Blundell MP, Brewin J, Thrasher A, Pule M, Amrolia PJ.  
574 Towards gene therapy for EBV-associated posttransplant lymphoma with  
575 genetically modified EBV-specific cytotoxic T cells. *Blood.* 2014;124(16):2514-  
576 2522.

577 34. Heslop HE, Slobod KS, Pule MA, et al. Long-term outcome of EBV-specific T-  
578 cell infusions to prevent or treat EBV-related lymphoproliferative disease in  
579 transplant recipients. *Blood.* 2010;115(5):925-935.

580 35. Wherry EJ, Kurachi M. Molecular and cellular insights into T cell exhaustion.  
581 *Nat Rev Immunol.* 2015;15(8):486-499.

582 36. Papadopoulou A, Gerdemann U, Katari UL, et al. Activity of broad-spectrum T  
583 cells as treatment for AdV, EBV, CMV, BKV, and HHV6 infections after HSCT.  
584 *Sci Transl Med.* 2014;6(242):242ra283.

585 37. Wang X, Berger C, Wong CW, Forman SJ, Riddell SR, Jensen MC.  
586 Engraftment of human central memory-derived effector CD8+ T cells in  
587 immunodeficient mice. *Blood.* 2011;117(6):1888-1898.

588 38. Klebanoff CA, Gattinoni L, Torabi-Parizi P, et al. Central memory self/tumor-  
589 reactive CD8+ T cells confer superior antitumor immunity compared with  
590 effector memory T cells. *Proc Natl Acad Sci U S A.* 2005;102(27):9571-9576.

591 39. Chung YL, Wu ML. Clonal dynamics of tumor-infiltrating T-cell receptor beta-  
592 chain repertoires in the peripheral blood in response to concurrent

593 594 595 596 597 598 599 600 601 602 603 604 605 606 607 608 609 610 611 612 613 614 615 616 617 618 619 620 621 622 623 624 625 626 627 628 629 630 631 632 633 634 635 chemoradiotherapy for Epstein-Barr virus-associated nasopharyngeal carcinoma. *Oncoimmunology*. 2021;10(1):1968172.

40. Wang G, Mudgal P, Wang L, et al. TCR repertoire characteristics predict clinical response to adoptive CTL therapy against nasopharyngeal carcinoma. *Oncoimmunology*. 2021;10(1):1955545.

41. Rosemarie Q, Sugden B. Epstein-Barr Virus: How Its Lytic Phase Contributes to Oncogenesis. *Microorganisms*. 2020;8(11).

42. Feng WH, Israel B, Raab-Traub N, Busson P, Kenney SC. Chemotherapy induces lytic EBV replication and confers ganciclovir susceptibility to EBV-positive epithelial cell tumors. *Cancer Res*. 2002;62(6):1920-1926.

43. Westphal EM, Blackstock W, Feng W, Israel B, Kenney SC. Activation of lytic Epstein-Barr virus (EBV) infection by radiation and sodium butyrate in vitro and in vivo: a potential method for treating EBV-positive malignancies. *Cancer Res*. 2000;60(20):5781-5788.

44. Grywalska E, Rolinski J. Epstein-Barr virus-associated lymphomas. *Semin Oncol*. 2015;42(2):291-303.

45. Ott PA, Dotti G, Yee C, Goff SL. An Update on Adoptive T-Cell Therapy and Neoantigen Vaccines. *Am Soc Clin Oncol Educ Book*. 2019;39:e70-e78.

46. Deng Y, Chatterjee B, Zens K, et al. CD27 is required for protective lytic EBV antigen-specific CD8+ T-cell expansion. *Blood*. 2021;137(23):3225-3236.

47. Tay RE, Richardson EK, Toh HC. Revisiting the role of CD4(+) T cells in cancer immunotherapy-new insights into old paradigms. *Cancer Gene Ther*. 2021;28(1-2):5-17.

48. Mautner J, Bornkamm GW. The role of virus-specific CD4+ T cells in the control of Epstein-Barr virus infection. *Eur J Cell Biol*. 2012;91(1):31-35.

49. Haque T, Wilkie GM, Jones MM, et al. Allogeneic cytotoxic T-cell therapy for EBV-positive posttransplantation lymphoproliferative disease: results of a phase 2 multicenter clinical trial. *Blood*. 2007;110(4):1123-1131.

50. Volk A, Hartmann S, Muik A, et al. Comparison of three humanized mouse models for adoptive T cell transfer. *J Gene Med*. 2012;14(8):540-548.

51. Rauser G, Einsele H, Sinzger C, et al. Rapid generation of combined CMV-specific CD4+ and CD8+ T-cell lines for adoptive transfer into recipients of allogeneic stem cell transplants. *Blood*. 2004;103(9):3565-3572.

52. Merlo A, Turrini R, Bobisse S, et al. Virus-specific cytotoxic CD4+ T cells for the treatment of EBV-related tumors. *J Immunol*. 2010;184(10):5895-5902.

53. Nowakowska J, Stuehler C, Egli A, et al. T cells specific for different latent and lytic viral proteins efficiently control Epstein-Barr virus-transformed B cells. *Cytotherapy*. 2015;17(9):1280-1291.

54. Khanna N, Stuehler C, Conrad B, et al. Generation of a multipathogen-specific T-cell product for adoptive immunotherapy based on activation-dependent expression of CD154. *Blood*. 2011;118(4):1121-1131.